Final Degree Thesis

Bachelors Degree in Industrial Technology

Simulation of a grid connected converter for PV application

Author: Alex Mons Cabré
Directors: Eduardo Prieto Araujo
José Montero Cassinello

Date: September 2019

Escola Tècnica Superior
d'Enginyeria Industrial de Barcelona

ABSTRACT

In this thesis, a model for a grid connected converter for a PV system is described and simulated.

A brief explanation of the main characteristics and how voltage source converters and photovoltaic systems work is made before presenting two models that describe the performance and behavior of a VSC and a PV array.

First, the models are presented in a theoretical framework, and then several simulations are carried out. Two different scenarios are presented in which diverse features of the converter model are shown, as well as presenting some applications for the PV model.

All the models and simulations are built and performed in Matlab and Simulink software.

INDEX

FIGURE INDEX

GLOSSARY

DC Direct Current

AC Alternating Current

PV Photovoltaic

LED Light-Emitting Diode

I-V Current-Voltage

P-V Power-Voltage

MPP Maximum Power Point

STC Standard Testing Conditions

LCC Line Commutated Converters

VSC Voltage Source Converter

PWM Pulse Width Modulation

MOSFET Metal Oxide Semiconductor Field Effect Transistor

IGBT Insulated Gate Bipolar Transistor

PI Proportional-Integral

1. PREFACE

1.1. Context

Development in demand response, energy optimisation and the reduction of the industry's carbon footprint are some of the many challenges that the utility industry is facing in the near future. All of these improvements cannot be obtained with the existing electricity grid.

The existing electrical grid is of a hierarchical nature in which power plants and generators are at the top, supplying all sorts of loads (industrial, domestic, etc.) which are at the bottom. The energy in the system has a one-way flow, from top to bottom of the chain.

In a fossil-fuel combustion dominated system, only one third of the fuel energy is converted into electricity and none of heat waste resulting from the combustion is recovered. Around 8% of the output energy is lost in the transmission lines. Furthermore, 20% of the generation capacity is only needed to reach peak demand, which is only in use for 5% of the time.

In the existing grid, unexpected raises in the demand can lead to system instability. With no safety margins, any unexpected surge in demand or anomaly can trigger a failure in the grid. Due to the hierarchical topology, the grid suffers from what can be called domino effect failures; a disturbance in the generation system can cause a failure in the end of the chain.

In order to overcome the problems associated to the conventional grid, utility companies are building towards a new approach, the smart grid [1].

Some of the main reasons why the transition from the conventional grid to the smart grid is necessary are:

- To provide better service quality.
- To reach the increasing energy demand caused by the rise of new technologies, such as electric vehicles.
- To integrate of renewable sources, such as solar or wind, into the system along with storage systems.
- To make the whole grid more efficient, cost-effective and environmentally friendly.

The fast rise of renewable technologies, such as photovoltaic and wind power, can not be explained without the development of power converters that allow the generated energy to be fed into the electricity grid [2].

1.2. Motivation

To complete my bachelor degree in Industrial Engineering, I wanted to find a project that enabled me to get a deeper understanding of a specific topic, especially in a degree where a lot of different subjects and fields are encompassed.

I found in this project the opportunity to learn more about power converters, which is a current issue in the energy sector. Doing research on a topic that contributes to energy sustainability and environmental protection is an added motivation for me, as I have always been intrigued and fascinated by new technologies that aim for a better and more efficient future in energy terms.

This project has also allowed me to extend my knowledge and experience with the software tools Matlab and Simulink, which I was introduced to during my degree.

2. INTRODUCTION

2.1. Objectives of the project

In this project, the modeling of a grid-connected PV array is approached.

The main objective is to understand the characteristics and operation of voltage source converters and obtain an accurate model in order to make simulations and study how the converter behaves in different situations of operation. Simulation is a much faster, safer and cost efficient alternative to experimental testing, so it is essential to have a reliable model that can be used as a first step for real installations of these kind of converters.

Another objective of this project is to present a method of modeling photovoltaic arrays. The main goal in this case is to obtain the parameters that define the current-voltage equation using the data provided by the manufacturers. Once this equation is obtained, it is possible to find the optimal working conditions for the arrays in any given meteorological condition.

Finally, a Matlab and Simulink model is presented and used for the simulation of two different scenarios that aim to exemplify the characteristics and behavior of the two explained models.

2.2. Scope of the project

This is an academic project, where the main outcome is understanding how to model a grid-connected PV array. A simulation of the model is made with the objective of comprehending how the model works and observing its behavior.

The project is made in a theoretical framework, there is no experimental validation for any of the results obtained. So the models presented in this project should not be used as a tool for the installation of a system in real life. Experimental testing needs to be done in order to validate the models and guarantee that they are completely reliable.

The idea of the models proposed in this project is for them to be used as a basis for further improvements and upgrades. In this way, the resulting models would be more complete and reliable, moreover, they would be helpful for other possible applications.

3. PHOTOVOLTAIC MODELING

A Photovoltaic system is a power system that converts sunlight into electricity. The most basic PV device is a cell, cells can be arranged to create panels and arrays. PV systems often consist of several components, such as solar panels, solar inverters, cables and mounting.

The output voltage and current of a PV panel can be directly used to supply small loads of DC nature, such as LEDs or DC motors without the need of any converter. However, for more complex applications, an electronic converter is needed in order to process the voltage and current given from the PV device. The converters are in charge of controlling and regulating the current, voltage and power exchange of the PV system.

3.1. Operation

A PV cell is essentially a diode that creates electricity when exposed to sunlight.

The cells consist of a thin layer of semiconductor, specially treated in order to create the p-n junction, a metallic grid is placed on the top side of the cell.

The photons received from the sunlight generate carriers in the p-n junction and if the two sides of the cell are short-circuited with a cable, then an electric current is obtained.

The rate of generation depends on different factors such as the incident light flux, the semiconductor band-gap, the reflectance and temperature of the surface, the carrier concentration of the semiconductor, the electronic mobility and the recombination rate.

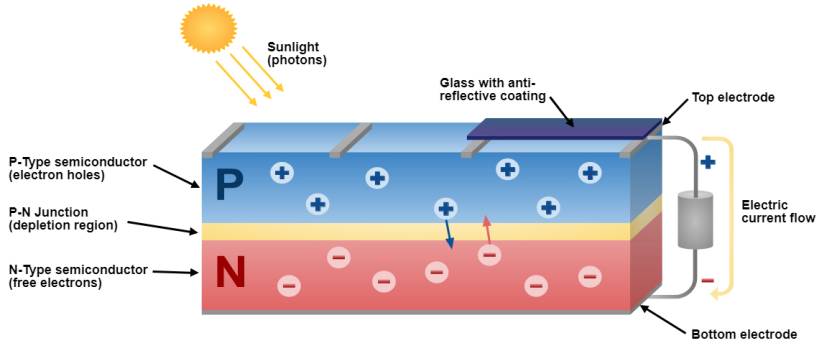

Figure 3.1.1. Basic PV Cell construction [3]

The incident radiation is composed of a range of energies, and each PV cell has its band-gap. The fraction of the radiation outside the band-gap is not useful to create electricity, it only contributes to generate heat in the cell.

Many materials can be used as semiconductors, among which Silicone is the most commonly used. It is not the most efficient material however, its manufacturing process is feasible in large scale.

The study of the physics of photovoltaic cells is complex. In this thesis, comprehending the electrical characteristics is enough for its modeling. The main objective for modeling a PV array is to obtain the parameters of the I-V equation using the data given by the manufacturer in the data-sheets and the PV panel five parameter model [5].

3.2. Modeling

The considered equivalent circuit for a PV cell, show in *Figure 3.2.1,* is represented by a current source in parallel with a diode, a parallel resistance Rp and a series resistance Rs, that model the existing losses in the cell. Other models are proposed in order to obtain more details, but the single diode model is found to be a simple yet highly accurate, so it is the one chosen to simply model and simulate PV devices [4].

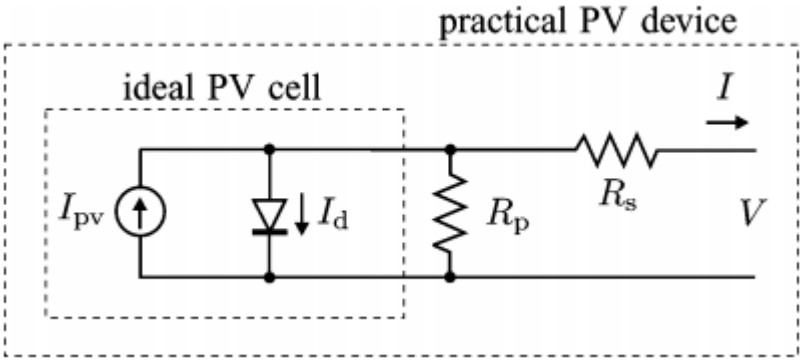

Figure 3.2.1. Single diode equivalent circuit of a PV cell [5]

The following equation describes the I-V curve of a PV array consisting on Ns cells connected in series and Np cells connected in parallel. A higher number of cells in series cause a higher voltage, while adding parallel cells contributes to higher currents.

$$I = I_{pv} - I_0\left[\exp\left(\frac{V + R_s I}{V_t a}\right) - 1\right] - \frac{V + R_s I}{R_p} \quad \textit{(Eq. 3.1)}$$

Where I_{pv} and I_0 are, respectively, the photovoltaic and saturation currents. $V_t = \frac{N_s k T}{q}$ *(Eq. 3.2)* is the thermal voltage, *q* is the electron charge, 1.60218×10−19 C, *k* is the Boltzmann constant, 1.38065×10−23 J/K, and T is the cell temperature in K. *a* is the diode ideality factor, which values vary from 1 to 1.5, so 1.3 is taken as an good value for the model. This equation generates the characteristic I-V curve shown in the following figure.

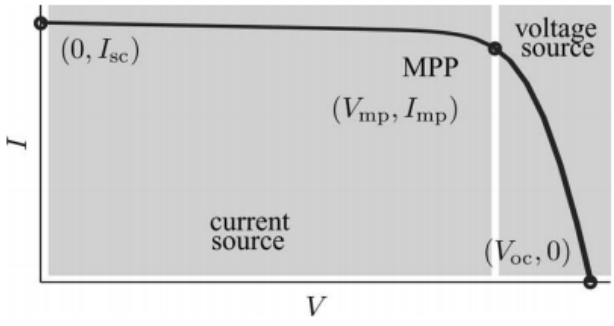

Figure 3.2.2. I-V curve for a PV panel with its three most remarkable points [5]

PV array data-sheets provided by the manufacturers contain a series of experimental electrical and thermal data that is not enough to adjust the model proposed previously; for example, there is no data of the PV current or the resistances.

In order to complete the model, the missing parameters will have to be obtained from equations that will later be presented, using the information provided in the data-sheets:

- Nominal open circuit voltage $V_{oc,n}$
- Nominal short-circuit current $I_{sc,n}$
- Voltage at the maximum power point (MPP) V_{mp}
- Current at the MPP I_{mp}
- Open circuit voltage temperature coefficient Kv
- Short-circuit temperature coefficient Ki
- Maximum peak output power $P_{max,e}$

All this information is referenced to the STC, standard test conditions of solar irradiation and cell temperature, that correspond to 1000 W/m2 and 25ºC.

The series resistance is low, and the parallel resistance is high, so the assumption that $I_{sc} \simeq I_{pv}$ is commonly made. The light-generated current is influenced by the temperature and the irradiance according to:

$$I_{pv} = \left(I_{pv,n} + K_I \Delta T\right) \frac{G}{G_n} \quad \textit{(Eq. 3.3)}$$

Where $I_{pv,n}$ is the PV current under STC conditions, $\Delta T = T - Tn$, with T_n and G_n being the nominal cell temperature and irradiance, 298 K and 1000 W/m2, while T and G are the cell temperature and irradiance, also in Kelvin and W/m2.

The saturation current I_0 is heavily dependent on the temperature and *Eq. 3.4* shows it.

$$I_0 = \frac{I_{sc,n} + K_I \Delta T}{exp\left(\frac{V_{oc,n} + K_V \Delta T}{aV_t}\right) - 1} \quad \textit{(Eq. 3.4)}$$

This equation has a different approach to the temperature dependence of the saturation current, according to the variation of the open-circuit voltage according to the voltage temperature coefficient Kv. This simplifies the model and minimizes the error in the I-V curve near the open-circuit point.

The values of R_s and R_p will be obtained in an iterative process. The method chosen consists in finding the values of R_s and R_p which make the maximum power calculated equal to the experimental maximum power given in the data-sheet $P_{max,e}$. By making $P_{max} = P_{max,e}$, the relation between R_s and R_p can be found:

$$R_p = \frac{V_{mp}\left(V_{mp} + I_{mp}R_s\right)}{V_{mp}I_{mp} - V_{mp}I_0\, exp\left[\frac{V_{mp} + I_{mp}R_s}{N_s a}\frac{q}{kT}\right] + V_{mp}I_0 - P_{max,e}} \quad \textit{(Eq. 3.5)}$$

Once knowing the value of the only remaining variable needed for *Eq. 3.1* , $I_{pv,n}$ can be calculated as the following equation shows:

$$I_{pv,n} = \frac{R_p + R_s}{R_p} I_{sc,n} \quad \textit{(Eq. 3.6)}$$

The algorithm shown in *Figure 3.2.3* is used to calculate all the parameters needed to define the I-V curve for the desired data-sheet information and different input temperature and irradiation conditions.

The process starts with $R_s = 0$ and increments it by a small amount in every iteration until it reaches a value where the calculated power is almost equal to the experimental value. The initial value of R_p to start the iterative process can be calculated with the following equation[5].

$$R_{p,min} = \frac{V_{oc,n} - V_{mp}}{I_{mp}} \quad \textit{(Eq. 3.7)}$$

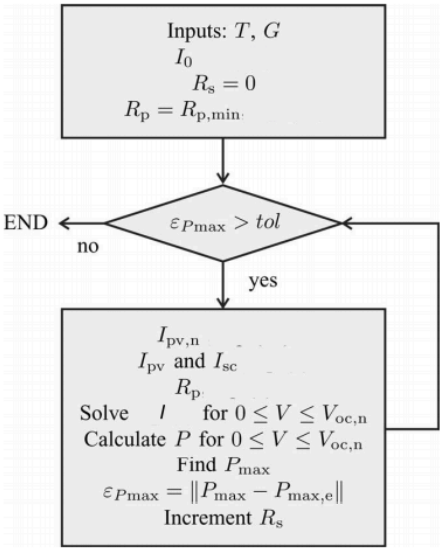

Figure 3.2.3. Scheme of the algorithm used to obtain the I-V curve [5]

3.3. Obtaining the I-V curve

In the next step, the concepts and criteria explained in the theoretical framework are applied to a practical situation in order to obtain the results of the case studied.

The algorithm is implemented in MATLAB. The script contains the information taken from the data-sheet of a PV module given by the manufacturer, the number of parallel and series modules that are desired to be installed, and the working conditions of temperature and irradiance.

With this information and the use of the algorithm, the I-V equation can be defined, hence the I-V and P-V curves for the desired PV array can be plotted. Note that the power can be obtained simply by multiplying current and voltage.

The proposed photovoltaic array that will be further used for the simulation of the converter consists of 120 *Canadian Solar CS6K-300MS* panels, each one with a nominal maximum power of 300 W. Branches of 20 panels will be arranged in parallel in order for the output voltage of the array to be in the range of the converter voltage. Six of those branches are organized in series in order to generate a total nominal power of 36 kW.

From the data-sheet, the necessary information can be taken, but the manufacturers only provide the data for one cell, and the desired curve is for the complete array, 120 cells in this case, so the suitable values need to be modified for the whole array. The data for both cases is shown in *Table 3.3.1* [6].

CS6K-300MS, 1 Cell		**CS6K-300MS, 20 cell branches in parallel and 6 branches in series**
Max,e	300 W	36000 W
Vmp	32.5 V	650 V
Imp	9.24 A	55.44 A
Voc.n	39.7 V	794 V
Isc,n	9.83 A	59.98 A
Kv	-0.29	-0.29
Ki	0.05	0.05
Ns	60	1200

Table 3.3.1. Data-sheet information for a single panel and the calculated values for the array

The algorithm obtains all the necessary parameters to complete the I-V equation, in this case, in the nominal conditions of cell temperature of 25ºC and irradiation of 1000 W/m2.

Rs	0.527 Ω
Rp	2750 Ω
Ipv	58.99 A
I0	1.452e-7 A

Table 3.3.2. Parameters of the I-V equation obtained from the algorithm

An experimental I-V plot for a single PV panel is also provided in the data-sheet, plotting the resulting I-V curve for a single panel and comparing it to the experimental one is a good way of validating the model before carrying on to other calculations. The validation can be made comparing *Figure 3.3.1* and *Figure 3.3.2.* Note that in this case, the curve given by the manufacturer is from a slightly different model, but the corresponding data is similar enough to validate at a glance.

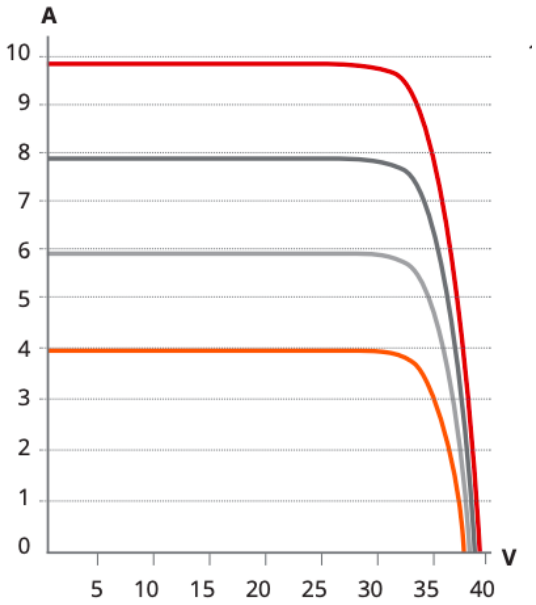

Figure 3.3.1. Data-sheet I-V curve for the CS6K-305MS panel, in red for STC [6]

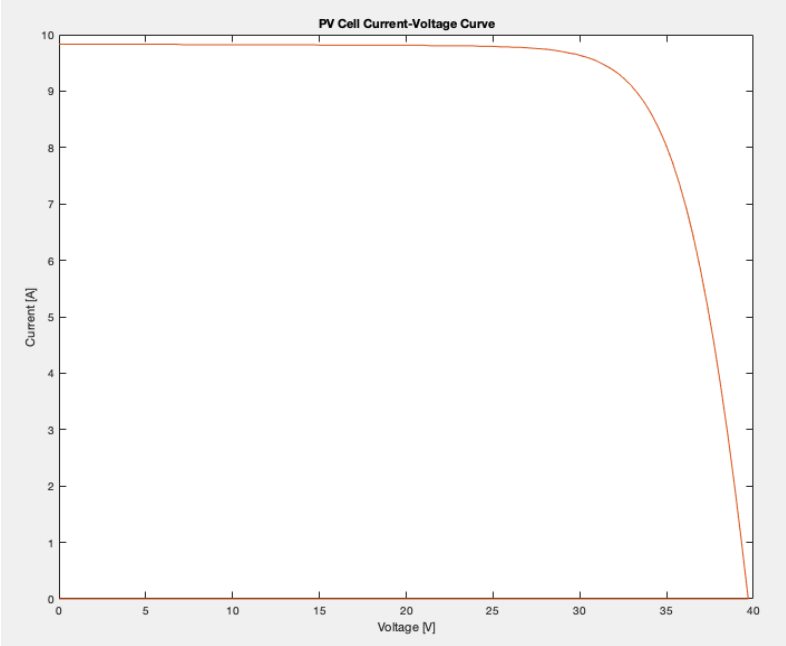

Figure 3.3.2. I-V curve for the CS6K-305MS panel obtained from the model under STC

Once the single panel I-V curve is validated, the Current-Voltage and Power-Voltage plots for the PV array under the given conditions are obtained.

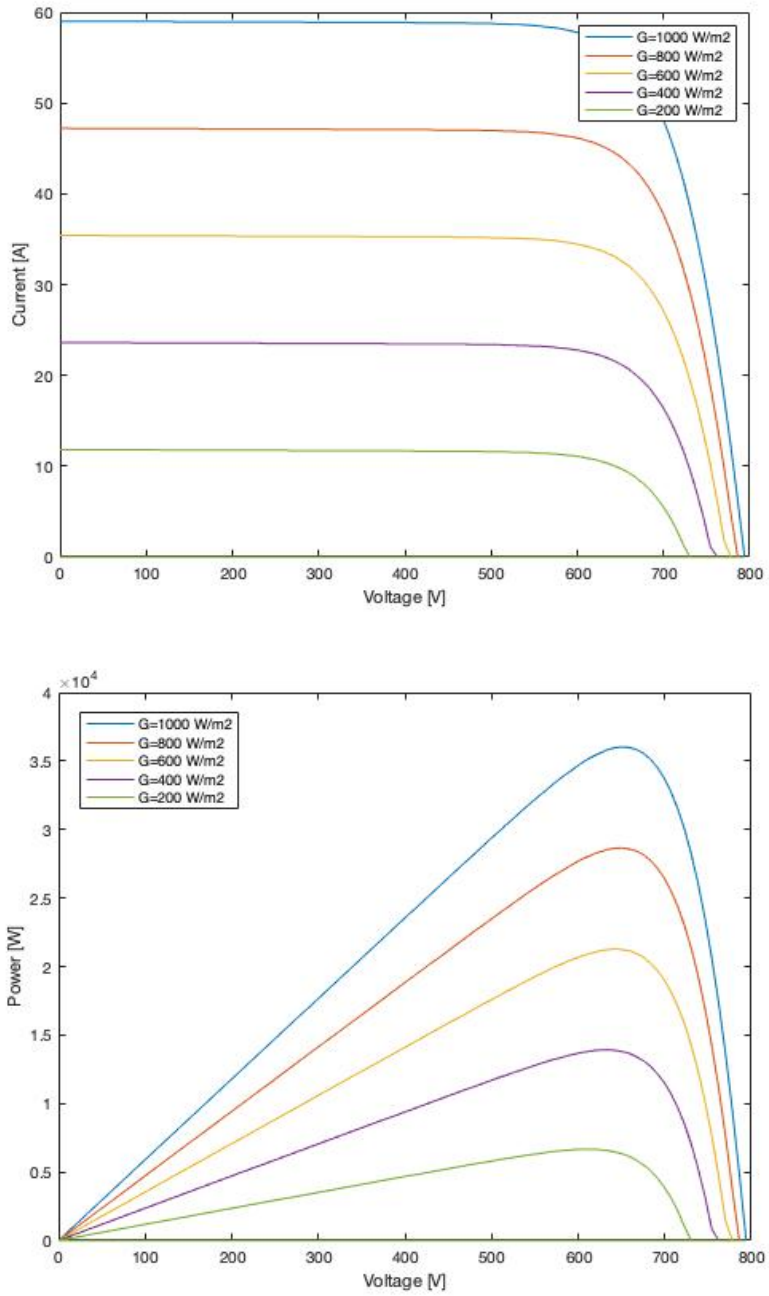

Figure 3.3.3. I-V and P-V curves for the CS6K-305MS panel under multiple conditions

As can be seen in the previous figures, the maximum power point for the PV array under STC is reached at a voltage of 650 V, at which the array generates a current of 65 A approximately. The I-V curve changes when the temperature and irradiance are modified.

STC conditions will be chosen for the most part in further simulations in this study. In one of the scenarios proposed, the weather conditions will change during the simulated period, but the variations in the curves due to weather changes are not considered essential when studying the behavior of the converter itself. The main objective of this chapter is to obtain the I-V and P-V curves of a specific PV array given certain temperature and irradiation conditions.

4. VOLTAGE SOURCE CONVERTER

The increasing use of renewable energy sources will require adequate integration into the modern grid.

Particularly, AC/DC converters with bidirectional power capability allow to integrate storage systems, wind turbines or PV into the conventional grid, creating micro-grids.

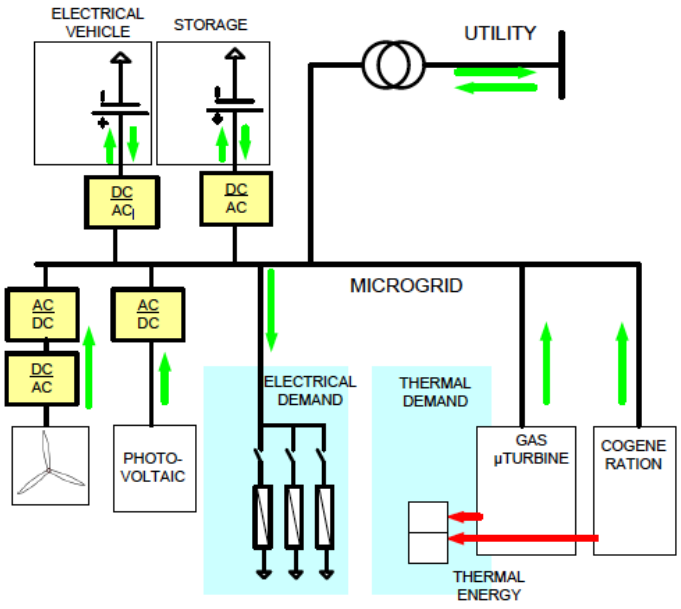

Figure 4.1. Example of a micro-grid with generation and storage systems [7]

The Voltage Source Converter essentially connects a DC device such as a battery or a PV cell to the AC three-phase grid. The converter applies voltages to the circuit enabling current flow, which can be imposed by changing the magnitude and phase of the voltages. The current flow establishes a power flow between different systems, in this case, between the DC PV system connected to the VSC and the grid. With the appropriate control, an optimal bidirectional power flow can be established [7] [8].

Voltage Source Converters use technologies such as MOSFETs or IGBTs that provide fast switching and are able to modulate any voltage within the system limitations. Those devices are completely controllable, meaning that the opening and closing of the devices can be fully controlled. Therefore, an independent active and reactive power control can be obtained. This is a very interesting feature of this kind of controller. In addition, being able to modulate any voltage permits the converter to create networks from the beginning, providing a black start of the network.

Another commonly used controller is the so-called Line Commutated Converters, based on thyristor or similar technologies. Some of the main drawbacks of the LCC compared to the VSC are that the devices are not completely controllable and the converter consumes non-controllable reactive power. Large filters are required to cancel the low frequency harmonics generated, while in VSC the filtering can be obtained with much smaller filters. The main advantage of the LCC filters is that they commute at a lower speed, similar to the grid frequency, resulting in lower commuting losses.

4.1. Converter Topologies

Another classification can be made considering the number of levels of the converter. The common technologies used are the two-level or the multi-level, that can be implemented in various ways. Two-level controllers are used for low voltage applications, leaving the multi-level technologies for the modulation of higher voltages.

Two-level converters are able to apply two voltage levels. Depending on which IGBT is on, the middle point is connected to the upper part or the lower part of the DC bus, resulting in an output of $\pm\frac{U_d}{2}$.

The switching frequency is in the range of kHz and can be controlled, as well as the ratio between the time that each one of the transistors is connected in every switching period. Controlling this ratio is done by the switching devices and it is called Pulse Width Modulation technique.

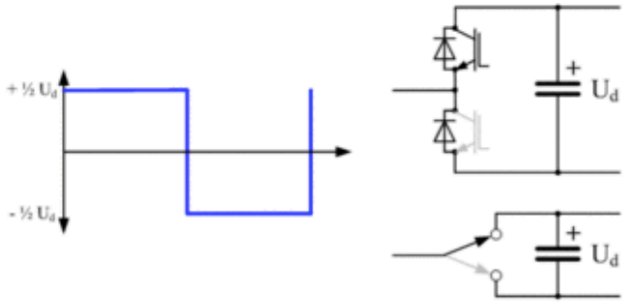

Figure 4.1.1. Operating principle of a 2-level converter [8]

Multi-level technologies allow the converter to work with higher voltages. By adding more IGBTs, more voltage levels can be obtained. The control is certainly more complex but the principle remains the same.

All the different topologies have the same objective of applying a desired sinusoidal voltage with PWM techniques and filtering the non-desired frequencies.

In order to simplify things, the IGBTs can be represented equivalently by three controlled voltage sources.

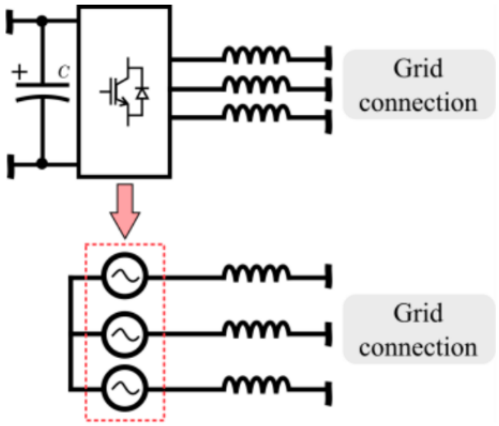

Figure 4.1.2. Modeling of the IGBTs in a VSC [8]

An inductor that acts like a low-pass filter and has to be implemented in order to cancel the high frequency harmonics introduced to the system by the PWM techniques.

This filtering avoids injecting high frequency current and voltage harmonics to the network, which can damage other devices connected. It is important to ensure a correct filtering in order to have a good integration of the devices using these converters.

4.2. System Description

The considered systems consists of a VSC converter connected to a three phase grid on one side, and connected to a storage system in the other side. The converter is basically composed of two sides: AC and DC side.

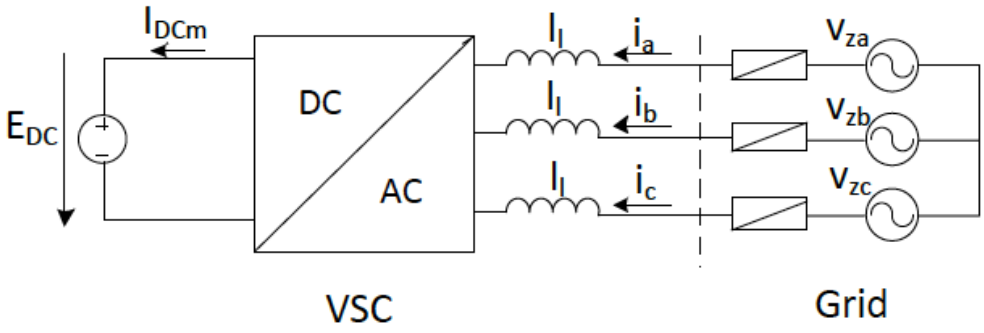

Figure 4.2.1. Diagram of a VSC with the DC side modeled as a voltage source [7]

The AC side can be represented by three controlled voltage sources, which simplify the IGBTs circuit.

An RL impedance, used as a low-pass filter, is located between the AC side of the converter and the grid connection. Apart from filtering the harmonics from the PWM, it enables to connect the grid and the VSC, both represented as voltage sources.

Since there is no reactive power in DC, the only power flowing through the DC side is active power. If a lossless model is considered, the active power exchanged with the AC side is equal to the power flowing through the DC side. A no losses model is considered in this case, although power losses could be added to the model if desired. The two sides of the converter, AC and DC are tied together by the active power exchanged, $P_{AC} = P_{DC}$.

The DC side is represented by a dependent current source that depends on the DC side voltage and power exchanged.

$$I_{DC} = \frac{P_{DC}}{V_{DC}} \quad \textit{(Eq. 4.1)}$$

The exchanged power is bidirectional, and even though in the model the AC and DC sides are decoupled, in reality, there is an electric connection every time an IGBT is closed, allowing currents to go through the system.

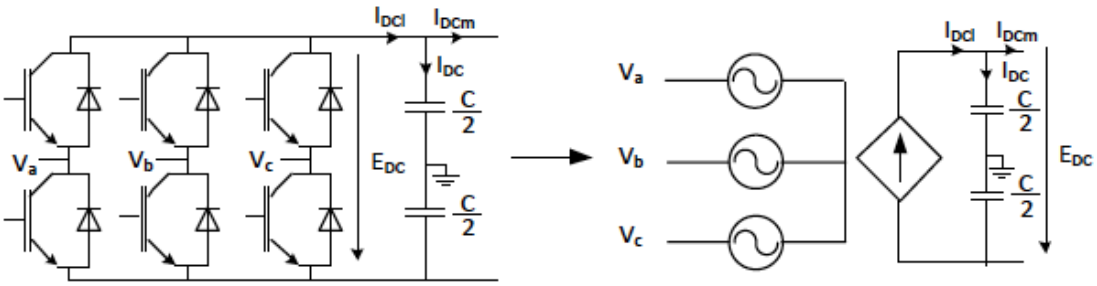

Figure 4.2.2. Model of the VSC [7]

A shunt capacitor C_{DC} is needed in the DC side of the converter. Its value affects different properties of the converter, such as the allowed DC voltage variation or the delay inferred in the filtering process. A good compromise can be accomplished setting the capacitor time constant between 40 and 50 ms. To calculate the capacitor size, the following formula is used.

$$C \geq \frac{\tau \Delta P_{DCmax}}{2V_{DC}\Delta V_{DCmax}} \quad \textit{(Eq. 4.2)}$$

Where τ is the capacitor time constant, ΔP_{DCmax} is the maximum DC power variation, V_{DC} is the DC bus voltage and ΔV_{DCmax} is the maximum DC voltage variation [9].

4.3. Mathematical Tools Used

In order de comprehend the operation of the technologies that will be later described, such as the PLL, certain mathematical transformations must be introduced. These transformations are implemented to simplify the operations and control of three phase sinusoidal variables, such as voltage or current.

The three-phase voltage in a balanced system is normally represented in an abc frame.

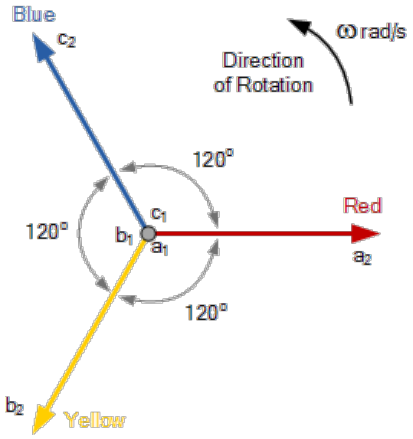

Figure 4.3.1. Three phase phasor diagram [10]

The moduli of the three phases are equal and the phases are 120º apart from each other.

The phase showed in the figure corresponds to the initial phase, the angular position of the three phases varies over time in relation to the frequency. The angular position or speed can be represented by the position of the rotating resulting vector.

For all the different cases that are going to be studied later on, the electrical grid will be considered stable and balanced.

4.3.1. Clarke Transform

Operations in the abc frame can be complex, so two mathematical transformations can be used in order to simplify the signals: the Clarke and Park transforms.

The Clarke transformation is a change of reference that transforms a three phase sinusoidal signal to a two phase sinusoidal signal, cancelling one of the three original variables in the case of a balanced system.

The phasors that were represented in natural reference frame ‘abc’, where the three phases are shifted 120º, are now shifted 90º. This corresponds to the *αβ0* axis, note that *0* axis is perpendicular to the *α-β* plane and its value in this reference is zero.

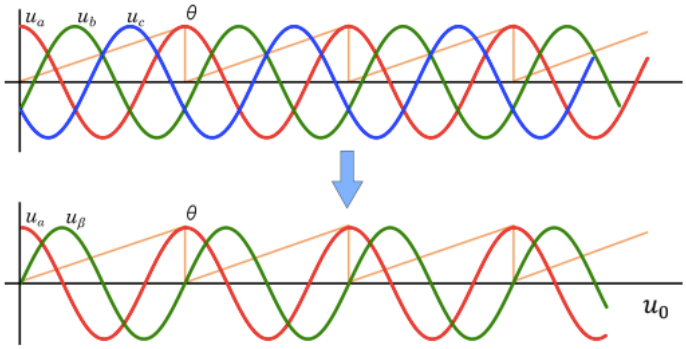

Figure 4.3.1.1. Time representation of voltages in abc and αβ domain [8]

The transformation is defined as:

$$[x_{\alpha\beta 0}] = [T_{\alpha\beta 0}][x_{abc}]$$

$$\begin{bmatrix} x_\alpha \\ x_\beta \\ x_0 \end{bmatrix} = \frac{2}{3} \begin{bmatrix} 1 & -\frac{1}{2} & -\frac{1}{2} \\ 0 & -\frac{\sqrt{3}}{2} & -\frac{\sqrt{3}}{2} \\ \frac{1}{2} & \frac{1}{2} & \frac{1}{2} \end{bmatrix} \begin{bmatrix} x_a \\ x_b \\ x_c \end{bmatrix}$$

(Eq. 4.3)

Where x_{abc} are the instantaneous electrical quantities expressed in the natural frame and $x_{\alpha\beta 0}$ are the transformed quantities in the new frame. x_0 is always zero for balanced systems.

It is a bidirectional transformation; its inverse form can be expressed as:

$$[x_{abc}] = [T_{\alpha\beta 0}]^{-1}[x_{\alpha\beta 0}] \quad \textit{(Eq. 4.4)}$$

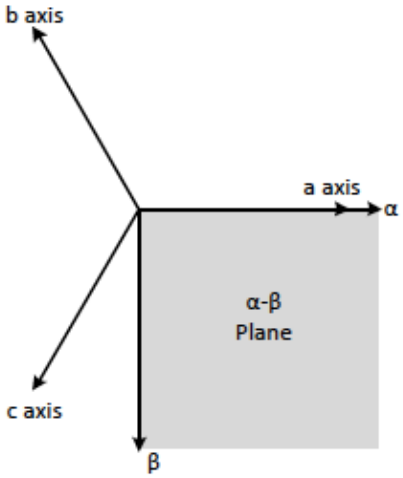

Figure 4.3.1.2. Geometrical representation of the abc and αβ planes [8]

4.3.2. Park Transform

To be able to use conventional control design, it is desired to have non-oscillatory variables. This can be accomplished by the Park transform. This transformation goes further than the Clarke's transform and it achieves even more simplified variables, cancelling their sinusoidal effect and turning them into constants.

The Park transform is a combination of the Clarke's transform and an angle rotation, corresponding to the electrical voltage angle. However, it can be applied in a single step.

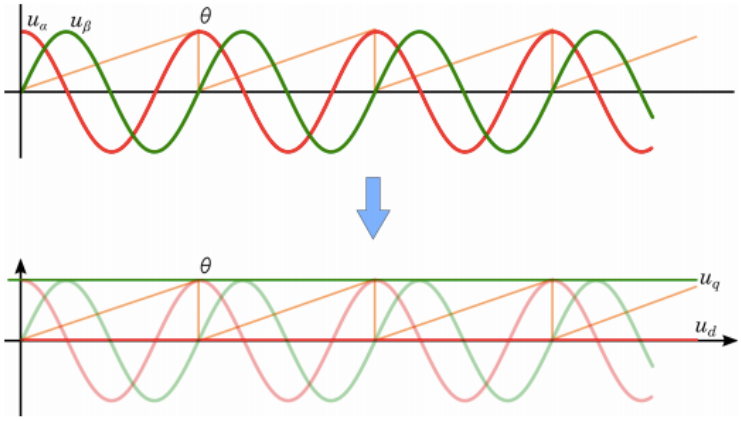

Figure 4.3.2.1. Time representation of voltages in αβ and qd domain [8]

The Park transform can be expressed as:

$$[x_{qd0}] = [T_{qd0}][x_{abc}]$$

$$\begin{bmatrix} x_q \\ x_d \\ x_0 \end{bmatrix} = \frac{2}{3} \begin{bmatrix} \cos\theta & \cos\left(\theta - \frac{2\pi}{3}\right) & \cos\left(\theta + \frac{2\pi}{3}\right) \\ \sin\theta & \sin\left(\theta - \frac{2\pi}{3}\right) & \sin\left(\theta + \frac{2\pi}{3}\right) \\ \frac{1}{2} & \frac{1}{2} & \frac{1}{2} \end{bmatrix} \begin{bmatrix} x_a \\ x_b \\ x_c \end{bmatrix}$$

(Eq. 4.5)

Where x_{qd0} are the variables in the synchronous reference frame *qd0*. x_0 is zero for balanced systems.

It is also a bidirectional transformation; its inverse is given by:

$$[x_{abc}] = [T_{qd0}]^{-1}[x_{qd0}] \quad \textit{(Eq. 4.6)}$$

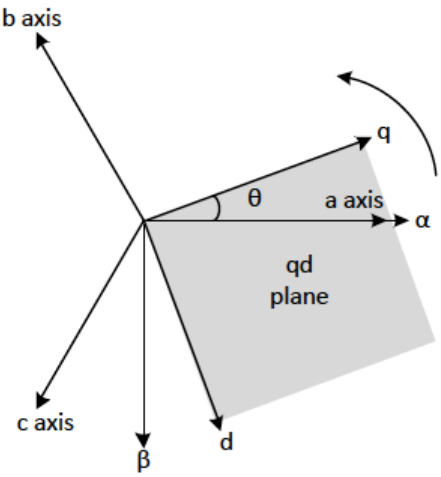

Figure 4.3.2.2. Geometrical representation of the abc, αβ and qd planes [8]

4.3.3. Instantaneous Power Theory

By transforming the voltage and current to the synchronous frame using Clarke's transformation, the phasors can be defined as [7]:

$$V_{qd} = \frac{v_q - jv_d}{\sqrt{2}} \quad \textit{(Eq. 4.7)}$$

$$I_{qd} = \frac{i_q - ji_d}{\sqrt{2}} \quad \textit{(Eq. 4.8)}$$

In a three-phased system, the power is:

$$S = P + jQ = 3V_{qd}I_{qd}{}^{*} = 3\left(\frac{v_q - jv_d}{\sqrt{2}}\right)\left(\frac{i_q + ji_d}{\sqrt{2}}\right) \quad \textit{(Eq. 4.9)}$$

The active and reactive power in the qd domain are expressed as:

$$P = \frac{3}{2}\left(v_q i_q + v_d i_d\right) \quad \textit{(Eq. 4.10)}$$

$$Q = \frac{3}{2}\left(v_q i_d + v_d i_q\right) \quad \textit{(Eq. 4.11)}$$

4.4. Control Scheme

Once seen the basic structure of the converter: the grid connection, the filter, the AC side, with its corresponding modulation techniques, and the DC side, this section will focus on the control scheme of the converter [7] [8].

The control of the converter is composed of different parts that together allow it to apply certain voltages in order for it to perform as desired.

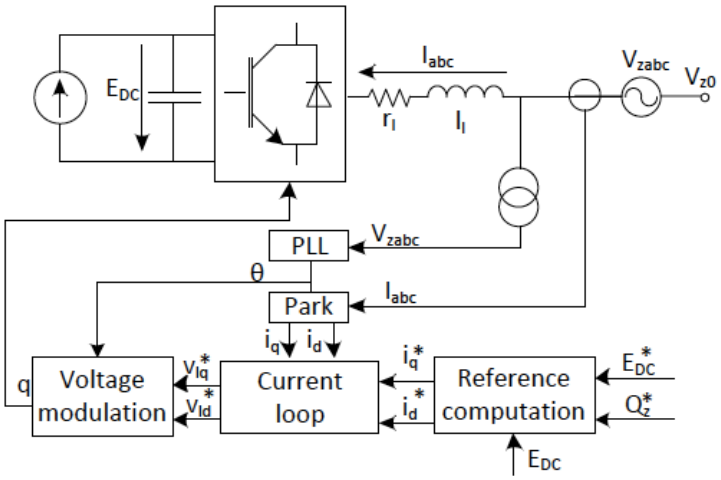

Figure 4.4.1. Diagram of the control scheme for the VSC model [7]

- The Phase Lock Loop measures the grid voltages and tracks the angle of the system as well as converting the voltages from *abc* domain to *qd0*.
- The Current Reference Computation calculates the reference currents given certain values of desired active and reactive power.
- The current set-points are used by the Current Loop, which controls the system currents to obtain desired voltage values, that enable the system to flow certain currents in order to obtain the desired power values.
- The Modulation is responsible of applying sinusoidal voltages from reference values of its magnitude, phase and frequency.

The control structure is operating overtime, constantly updating values.

The current loop defines the inner loop, which is the lower part of the control structure, which operates faster than the outer loop.

The outer loop defines the mode in which the converter is going to be functioning. Different operating modes could be:

- Control of the active power
- Control of the reactive power
- DC voltage regulation

In this specific case, the converter will be operating to control the DC voltage. Therefore, the active power exchanged in the AC side is going to be linked to the DC voltage.

Once all the different parts that compose the control structure of the converter have been briefly introduced, each part of the converter control is explained more in detail below.

4.4.1. Phase Lock Loop

The PLL is an essential part of the converter control. Its main purpose is to track the grid angle.

Once the angle of the grid is known, it is possible to apply the Park transformation that allows to switch from the abc domain into the *qd0* domain, where basic control principles can be applied to regulate the system.

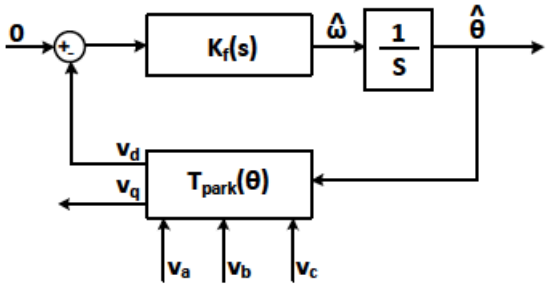

Figure 4.4.1.1. Phase Lock Loop block diagram [7]

To begin with, the grid voltage has to be measured, it can be done between phases or phase to neutral. Given the grid voltages in the *qd0* frame and the grid angle, the transformation can be applied and now the voltages turn into constant values in the *qd0* frame.

The control tracking structure consists in a closed loop system where the control variable is the *d* component of the voltage, which set-point is zero. This signal is compared to the set-point and its error is then filtered by a PI controller. The output of the PI controller is the angular velocity of the grid ω. The angle of the grid θ can be obtained by integrating the velocity.

The PI controller transfer function is defined as $C_{PI}(s)$ and its parameters τ_{PLL} and K_p can be obtained solving the system formed e*quations 4.12*, *4.13* and *4.14* :

$$C_{PI}(s) = \frac{\frac{1}{\tau_{PLL}} + s}{s} \quad \textit{(Eq. 4.12)}$$

$$\omega_n = \sqrt{\frac{K_p E_m}{\tau_{PLL}}} \quad \textit{(Eq. 4.13)}$$

$$\xi = \frac{\sqrt{\tau_{PLL} K_p E_m}}{2} \quad \textit{(Eq. 4.14)}$$

The feedback loop allows the PLL to keep track of any deviation in the grid frequency by accelerating or decelerating the rotation of the reference frame.

The output signals of the PLL are the grid angle θ and the voltage values v_{qd0}. θ will be also used in other transformations in the model.

4.4.2. Current Loop

The Current Control Loop is a necessary part of the system in charge of controlling the current flowing through the converter in order to exchange the desired active and reactive power. Currents can be controlled in different ways but it is preferred to work in the *qd0* domain, as the control becomes much more simple and easy than it would be in *abc*.

An important feature of the Current Loop is that active and reactive power can be controlled independently with the *q* and *d* components of the current respectively. This can be achieved by decoupling the *q* and *d* components with a Decoupling Loop that is added to the Current Loop.

Considering that the neutral can be removed from the equations, the voltage equations of the system are:

$$v_{z,abc} - v_{l,abc} = \begin{bmatrix} r_l & 0 & 0 \\ 0 & r_l & 0 \\ 0 & 0 & r_l \end{bmatrix} i_{abc} + \begin{bmatrix} l_l & 0 & 0 \\ 0 & l_l & 0 \\ 0 & 0 & l_l \end{bmatrix} \frac{d}{dt} i_{abc} \quad \textit{(Eq. 4.15)}$$

Using the Park transform, the equations can be transformed from abc to qd0.

$$T(\theta)v_{z,abc} - T(\theta)v_{l,abc} = T(\theta)\begin{bmatrix} r_l & 0 & 0 \\ 0 & r_l & 0 \\ 0 & 0 & r_l \end{bmatrix} i_{abc} + T(\theta)\begin{bmatrix} l_l & 0 & 0 \\ 0 & l_l & 0 \\ 0 & 0 & l_l \end{bmatrix} \frac{d}{dt} i_{abc} \quad \textit{(Eq. 4.16)}$$

$$v_{z,qd0} - v_{l,qd0} = \begin{bmatrix} r_l & 0 & 0 \\ 0 & r_l & 0 \\ 0 & 0 & r_l \end{bmatrix} i_{qd0} + T(\theta)\begin{bmatrix} l_l & 0 & 0 \\ 0 & l_l & 0 \\ 0 & 0 & l_l \end{bmatrix} \frac{d}{dt}\left(T(\theta)^{-1} i_{qd0}\right) \quad \textit{(Eq. 4.17)}$$

$$\begin{bmatrix} v_{z,q} \\ v_{z,d} \end{bmatrix} - \begin{bmatrix} v_{l,q} \\ v_{l,d} \end{bmatrix} = \begin{bmatrix} r_l & l_l\omega_e \\ -l_l\omega_e & r_l \end{bmatrix} \begin{bmatrix} i_q \\ i_d \end{bmatrix} + \begin{bmatrix} l_l & 0 \\ 0 & l_l \end{bmatrix} \frac{d}{dt} \begin{bmatrix} i_q \\ i_d \end{bmatrix} \quad \textit{(Eq. 4.18)}$$

As can be seen, there is a coupling between *q* and *d* magnitudes, since the matrix is not diagonal. So another loop is introduced in order to decouple the system, the decoupling loop.

For the decoupling loop, the following expressions are defined. The PLL imposes $v_{z,d} = 0$ as it is oriented with the *d* axis.

$$\begin{bmatrix} v_{l,q} \\ v_{l,d} \end{bmatrix} = \begin{bmatrix} -\hat{v_{l,q}} + v_{z,q} - l_l\omega_e i_{l,d} \\ -\hat{v_{l,d}} + l_l\omega_e i_{l,q} \end{bmatrix} \quad \textit{(Eq. 4.19)}$$

Finally obtaining two completely decoupled equations for the current control loop, the *q* component of the voltage is only affected by the *q* component of the current, and the same happens for *d* magnitudes.

$$\begin{bmatrix} \hat{v_{l,q}} \\ \hat{v_{l,d}} \end{bmatrix} = \begin{bmatrix} r_l & 0 \\ 0 & r_l \end{bmatrix} \begin{bmatrix} i_q \\ i_d \end{bmatrix} + \begin{bmatrix} l_l & 0 \\ 0 & l_l \end{bmatrix} \frac{d}{dt} \begin{bmatrix} i_q \\ i_d \end{bmatrix} \quad \textit{(Eq. 4.20)}$$

Once seen the voltage equations in time, Laplace is applied to them in order to implement the control. Note that a derivative in time is a multiplication by *s* in Laplace. The resulting equations in the new domain are:

$$\frac{i_q(s)}{\hat{v_{l,q}}(s)} = \frac{1}{l_l \cdot s + r_l} \quad \textit{(Eq. 4.21)}$$

$$\frac{i_d(s)}{\hat{v_{l,d}}(s)} = \frac{1}{l_l \cdot s + r_l} \quad \textit{(Eq. 4.22)}$$

A technique called Internal Model Control is utilized to cancel the internal dynamics of the plant and impose the desired dynamics for the system. The plant, equivalent to the filter, is a first order system, so it can be regulated with a classic PI controller.

Given the plant:

$$G(s) = \frac{1}{l_l \cdot s + r_l} \quad \textit{(Eq. 4.23)}$$

The parameters of the controller are defined in order to impose the wanted dynamics.

$$C_{PI}(s) = \frac{K_P \cdot s + K_I}{s} \quad \textit{(Eq. 4.24)}$$

K_P constant relates to the inductance value *l* of the plant and K_I relates to the resistance r_l. The time constant τ defines the transient response of the system, it corresponds to the time that the response will take to achieve 63% of its final value. τ is the same for each constant, and its value is usually defined 10 times faster than the converter switching frequency.

$$K_P = \frac{l_l}{\tau} \quad \textit{(Eq. 4.25)}$$

$$K_I = \frac{r_l}{\tau} \quad \textit{(Eq. 4.26)}$$

Two controllers are defined independently for *q* and for *d*. As mentioned before, a decoupling loop needs to be added to in order to independently control active and reactive power.

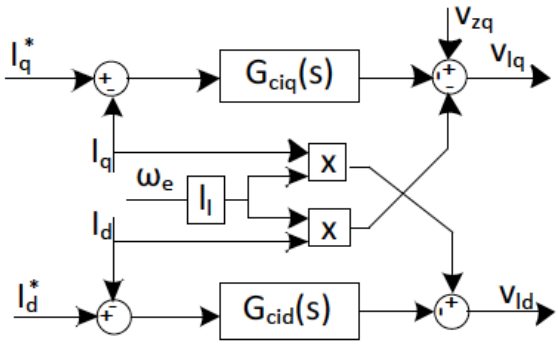

Figure 4.4.2.1. Block scheme of the Current Control Loop [7]

4.4.3. Current References Computation

The power expressions in the *qd* frame were introduced previously in *Figure 4.10* and *Figure 4.11*. Now considering $v_d = 0$, it is clear that the active and reactive power are only dependent on the *q* and *d* currents, respectively, and the current references can be obtained.

$$i_q{}^* = \frac{2}{3}\frac{P^*}{v_{z,q}} \quad \textit{(Eq. 4.27)}$$

$$i_d{}^* = \frac{2}{3}\frac{Q^*}{v_{z,q}} \quad \textit{(Eq. 4.28)}$$

The VSC controller presents various modes of operation, in the studied case, the DC voltage control is the option chosen for the control, while directly controlling the reactive power.

The *q* component of the current i_q is responsible of controlling the DC voltage. In order to obtain reference for the Current Loop, a DC Voltage Regulator is required.

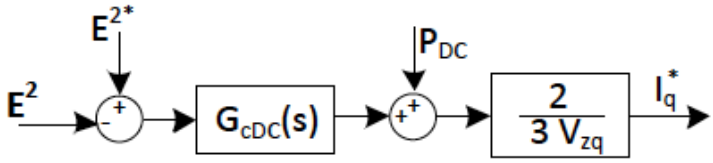

Figure 4.4.3.1. Block scheme of the DC Voltage Regulator [7]

It consists in a feed-forward arrangement that controls the squared DC Voltage, proportional to the energy stored in the capacitor. This signal is compared to the desired DC Voltage value and then controlled with a PI Controller, which gains can be calculated by:

$$C_{PI} = K_P + \frac{K_I}{s} \quad \textit{(Eq. 4.29)}$$

$$K_P = C\xi_E\omega_E \quad \textit{(Eq. 4.30)}$$

$$K_I = \frac{C\omega_E^2}{2} \quad \textit{(Eq. 4.31)}$$

The output P_C of the PI controller is the power that goes through the DC capacitor, thus the power reference P^* is:

$$P^* = P_C + P_{DC} \quad \textit{(Eq. 4.32)}$$

Where P_{DC} is the measured power of the DC side of the converter. Once P^* is known, $i_q{}^*$ can be directly obtained using *Eq. 4.27*.

4.5. Converter Model

A model of the Voltage Source Converter explained in this chapter is implemented in Matlab's Simulink. This allows to experiment with the VSC features and have a better understanding on how the controller works. The SIMSCAPE library is been used to add the electrical components of the circuit to the model.

Building the model is a helpful way of comprehending all the parts that compound the model, and the way it operates. While building it, it can be seen how changes in each of the different parameters affect the converter behavior.

A general view of the complete converter model is shown in *Figure 4.5.1.* Each one of the parts that conform the VSC are explained in detail below.

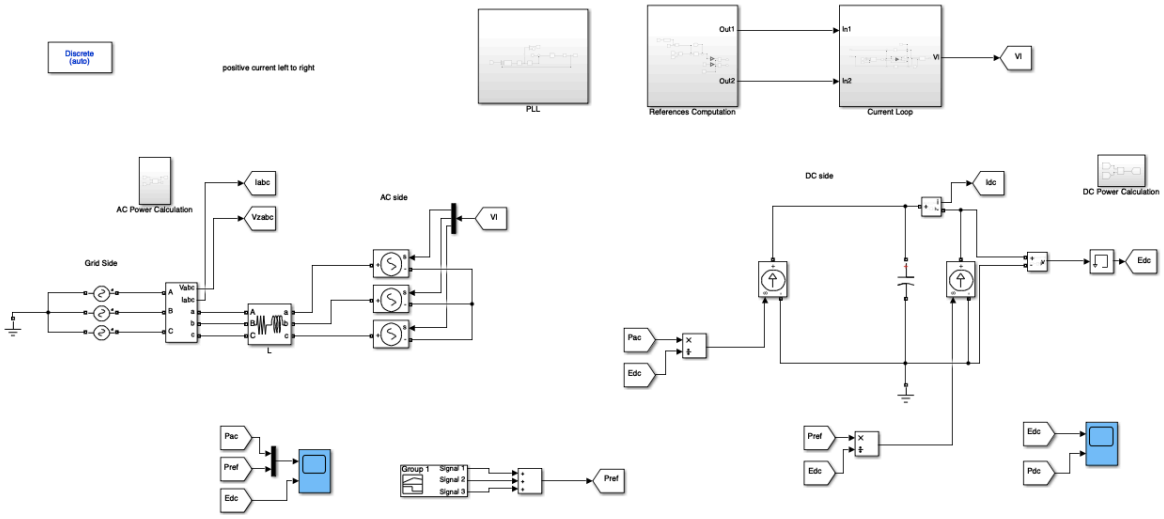

Figure 4.5.1. Overview of the VSC Simulink model

The grid is modeled as three AC voltage sources with a peak phase to neutral voltage of $400\frac{\sqrt{2}}{\sqrt{3}}$ V, each phase shifted 120º from each other.

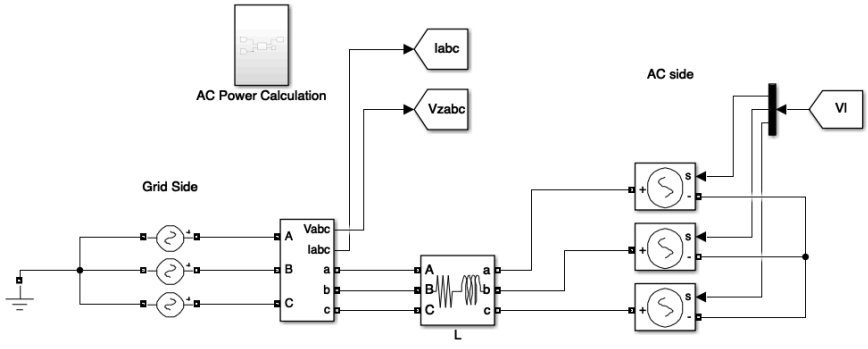

Figure 4.5.2. AC side of the converter Simulink model

The AC side of the converter consists of a RL series branch for each of the three phases and three controlled voltage sources. The values for the coupling resistances and inductances are 0.5 Ω and 5.4 mH [7].

The DC side is not electrically connected to the AC side, so the connection between both parts is made by a controlled DC current source, which imposes a current in the DC side. The current value is calculated so the power going through the DC part of the converter is equal to the active power exchanged between the converter and the grid in the AC side.

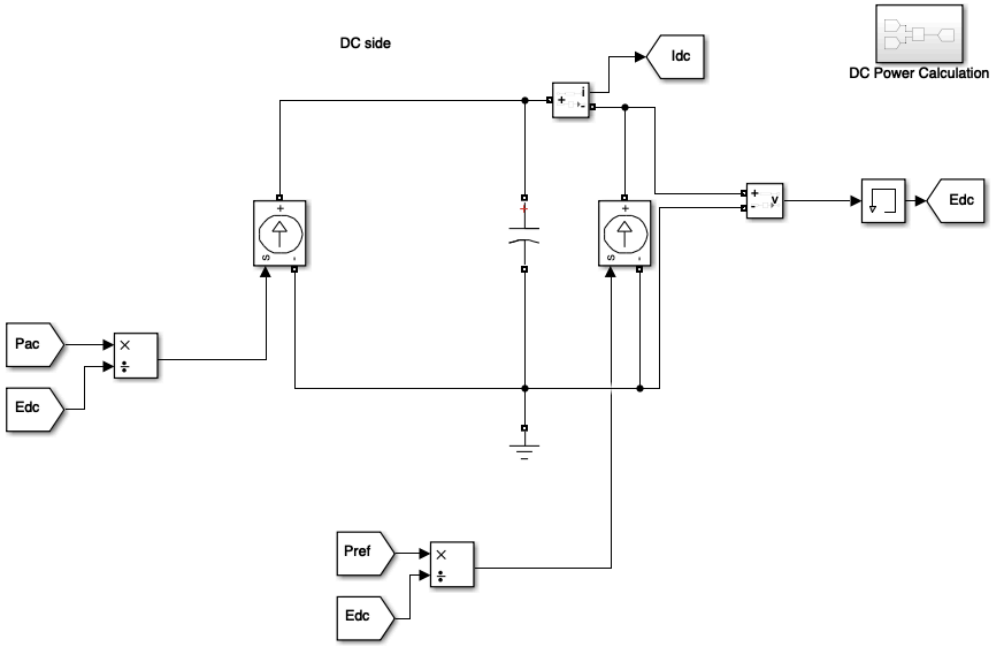

Figure 4.5.3. DC side (Simulink model)

The shunt capacitor takes a value of 1020 μF. Finally, another controlled current source is implemented in order to model the connection to the PV array output. This current source imposes the generated power in the DC side. Both the DC voltage and current are measured as they are needed for other calculations in the converter control. In *Figure 4.5.3*, a subsystem that calculates the DC power can be observed.

Continuing with the system description, the control loops implemented in the model are described. First, voltage and current measurements are taken from the AC side of the converter, as it can be seen in *Figure 4.5.2.* The first of these measurements is an input for the PLL, that transforms the voltages to the *qd0* frame by applying the Park transformation and tracks the grid angle. The outputs of the PLL, v_{zq} and θ will be used later in other parts of the control.

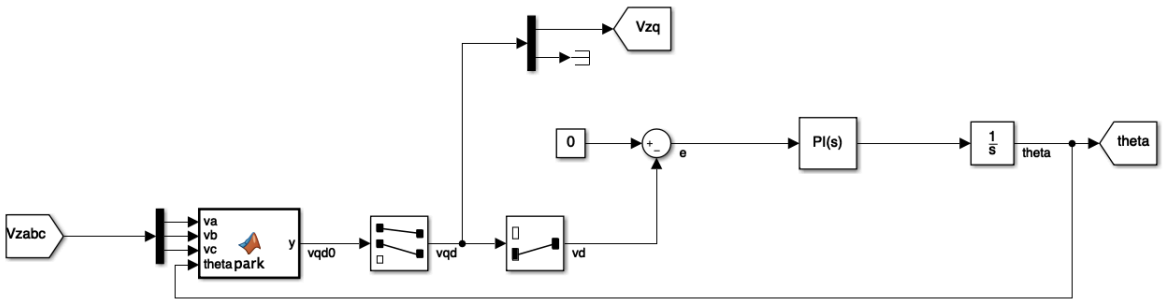

Figure 4.5.4. Phase Lock Loop (Simulink model)

The Current References Computation takes as inputs the active power reference, the PV array Power-Voltage curve approximation for the given weather conditions, the DC voltage, the DC power and the AC voltage as well as the set-point for the reactive power.

Given the power wanted to exchange by the converter, the corresponding DC voltage is calculated, since the P-V curve of the PV array is known. This value is used as the set-point for the DC bus voltage. The output of the loop is the DC power reference P^*, and together with the reactive power reference, the two current set-points are obtained.

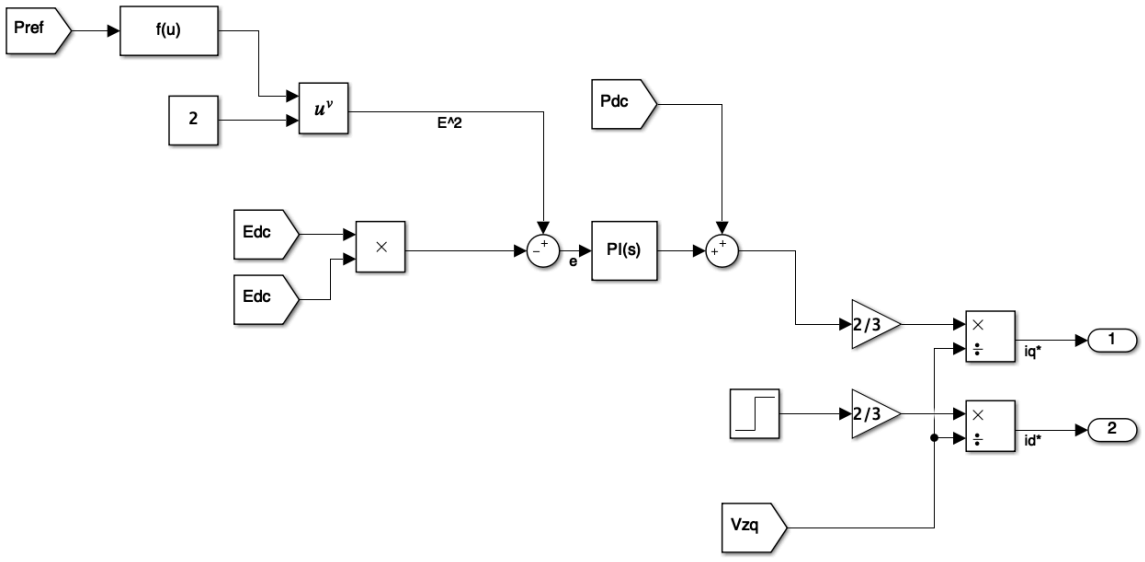

Figure 4.5.5. Current References Computation (Simulink model)

For the Current Loop, the Park transformation has to be applied again, this time for the currents measured in the three phases. It can be seen that the angle obtained in the PLL is now used here. The decoupling loop is added so active and reactive power can be controlled independently, as it was explained previously. The voltages obtained from the loop are in the *qd* frame, so it is necessary to transform they back to time domain with the inverse Park transform. The output voltage is used by the controlled voltage sources in the AC side in order to flow the desired amount of current through the converter, closing the control loop.

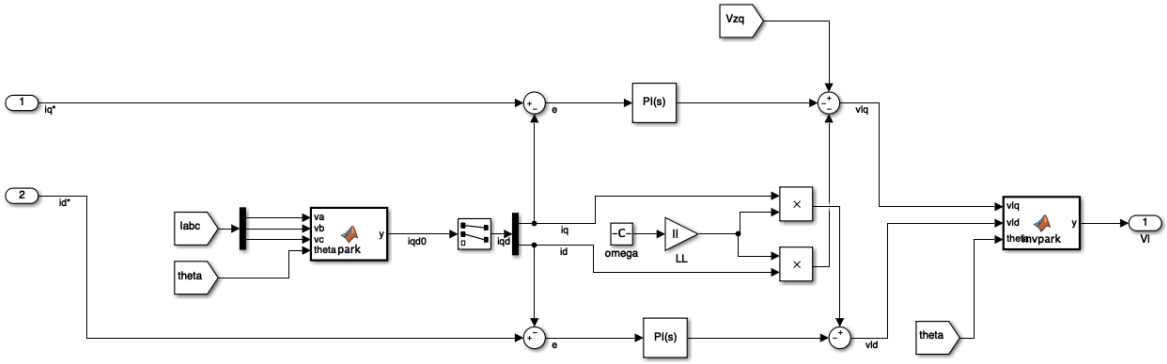

Figure 4.5.6. Current Loop (Simulink model)

5. SIMULATION

All the simulations will be performed in MATLAB and SIMULINK, the results will be visualized in the same interface.

Now that the model is completed and all its details explained, it is time to proceed to simulate some different situations. Using both the Voltage Source Converter and the PV array models, simulations will be carried out to observe and comprehend how both models function under different conditions. The cases that will be performed are described below.

5.1. Scenario 1

In this first case, weather conditions will not change during the course of the simulation, cell temperature and irradiance will remain constant, meaning that the PV array Current-Voltage curve obtained from the first model will be only one.

The interest in this case is to study how the VSC behaves when the following sequence of requirements are requested:

- Initially, no power is injected to the grid.
- At t=0.2 s, once steady state is reached, the maximum power generated by the PV array will be extracted and delivered to the grid.
- Again, after reaching steady state, a curtailment situation will be simulated, where the PV plant is asked to reduce its output power to a level below its full capability.
- At last, the complete available generated power will be again applied.

5.2. Scenario 2

Next, a new simulation scenario is defined. In this particular case, the weather conditions will change within the simulation period, replicating a real situation where a cloud would cover the PV panels from the sun. In this case, the irradiation and the cell temperature will drop during a certain amount of time, modifying the form of the I-V curve. During all the simulation the power supplied will be the maximum power available to be generated in the current weather conditions.

The simulation sequence for this scenario will be:

- Initially, STC are considered.
- After 0.2 seconds of simulation, the conditions are changed to 500 W/m2 and 20ºC.
- Finally, the conditions are set back to STC, simulating that the cloud has gone by and the situation is again the initial one.

5.3. Simulation Results

5.3.1. Scenario 1

First, the I-V and P-V curves for the STC are acquired. It is convenient to simplify the model by linearizing the curve in the zone of voltages in which the converter will be working. This step is not indispensable, but it simplifies the simulink model and the results, in practical terms, are not affected by this adjustment.

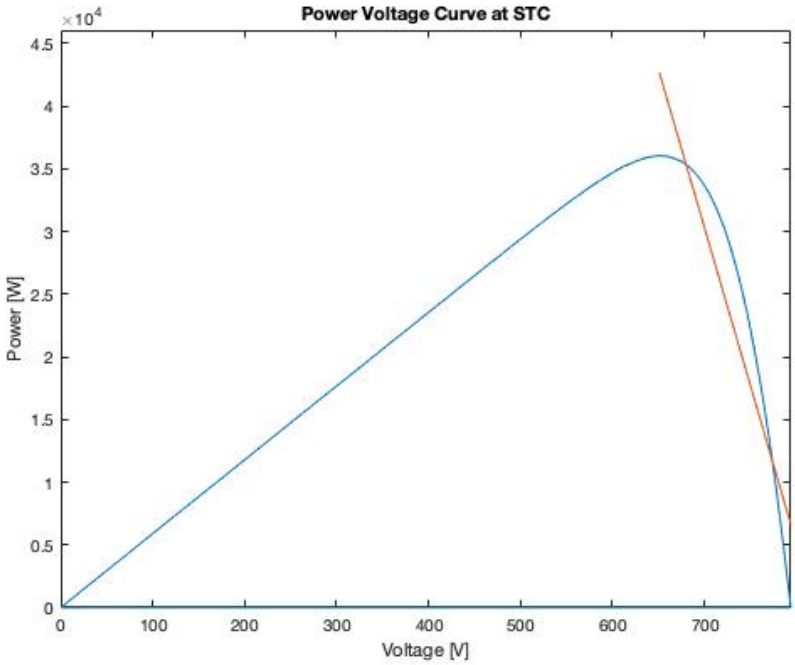

Figure 5.3.1.1. Power-Voltage Curve under STC and simplified line

The linear equation, obtained from linearizing data extracted from the desired region of the curve, is:

$$P = -251.95\ V + 206683\ [W] \quad \textit{(Eq. 5.1)}$$

The main inputs in this simulation case are the desired values of active power to be exchanged from the PV array to the grid. These values are shown in *Table 5.3.1.1*.

Time [s]	Desired Active Power [kW]
0 - 0.2	0
0.2 - 0.4	36
0.4 - 0.6	28
0.6 - 0.8	36

Table 5.3.1.1. Active power input values for the first simulation scenario

Both the P-V equation and the desired power are introduced in the Simulink converter model. Therefore, the simulation can be carried out.

In this simulation, the converter functions in three different working points, the first one when there is no power exchanged to the grid, and the other two in different points in the P-V simplified curve. Next, the behavior of the converter is analyzed.

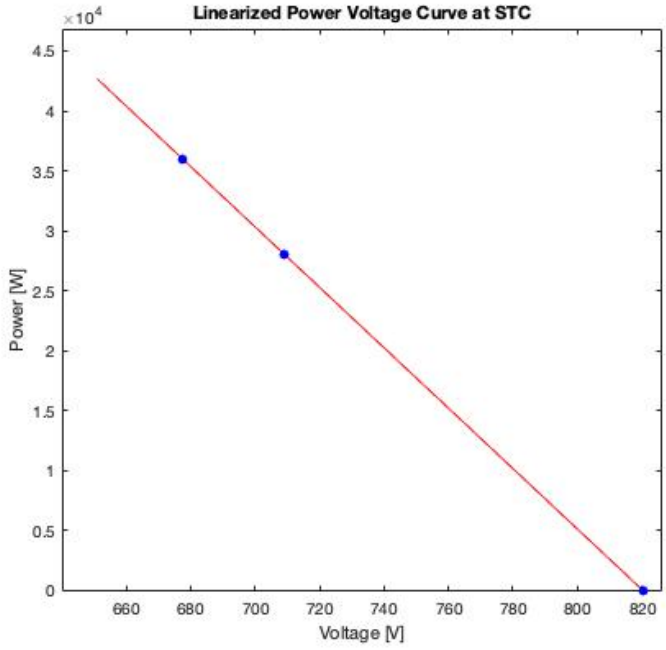

Figure 5.3.1.2. Linearized Power-Voltage curve under STC

The active power exchanged and its reference values are illustrated in *Figure 5.3.1.3*. The power set-point varies as a step signal and the exchanged power behaves as a second order response, converging to the desired value. Therefore the steady state error for the power is zero. *Figure 5.3.1.4* shows a more detailed view of the transient state, it can be observed that the final value is reached relatively fast.

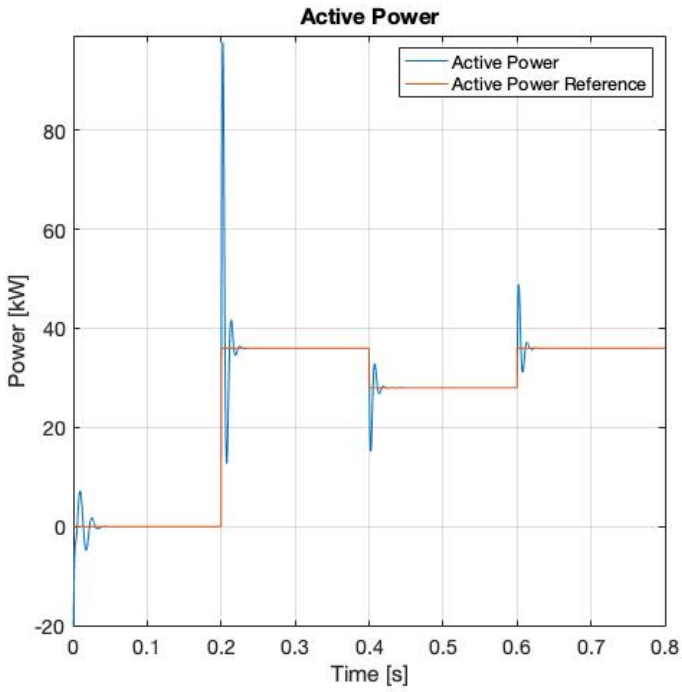

Figure 5.3.1.3. Evolution of the active power throughout the simulation

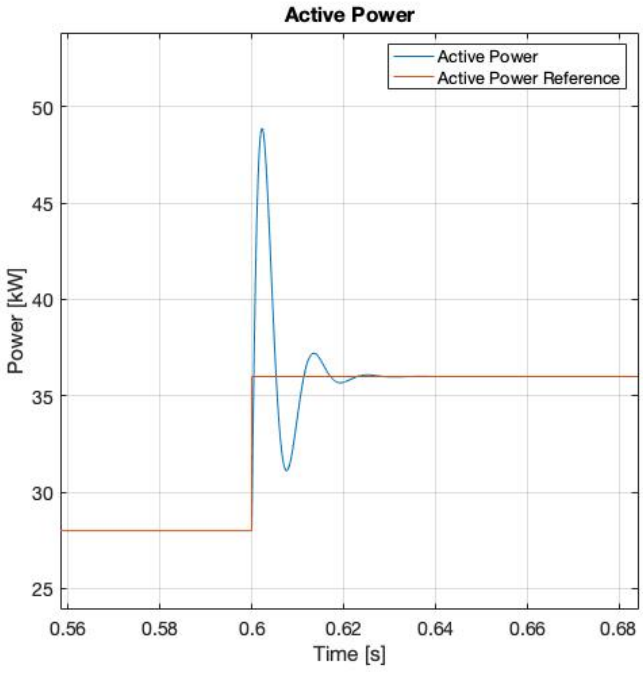

Figure 5.3.1.4. Detailed view of the transient state of the active power signal

The following figure shows DC bus voltage variation throughout the simulation. This magnitude changes every time a new power reference value is introduced to the system. The voltage values corresponding to each working point are given by the simplified P-V equation found previously. Here it can be seen that the converter can control the DC bus voltage so it guarantees that the PV array connected to the DC side is working in optimal conditions.

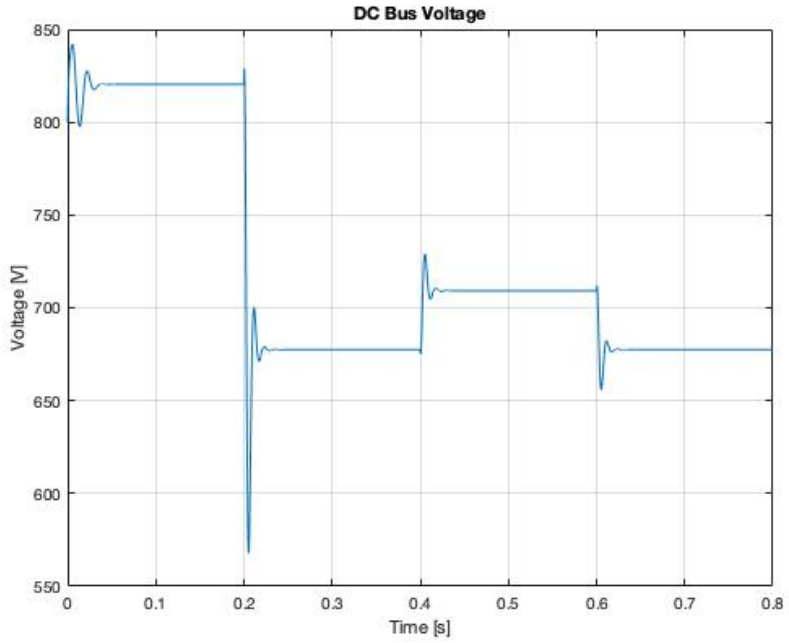

Figure 5.3.1.5. Evolution of the DC bus voltage throughout the simulation

By knowing the P-V curve and being able to modify the voltage, it is possible to set the PV array to any requested performance point, and this is exactly what is happening in this simulation.

- First, a new active power set-point is given, this value always has to be adequate to the generation capabilities of the device connected to the DC side of the converter.
- Then, using the P-V equation, it is found which voltage has to be imposed to the DC voltage in order for the PV array to generate this exact amount of power in the current meteorological conditions.
- Finally, the converter imposes the calculated voltage to the DC bus, allowing the solar array to generate and flow the desired power through the converter to the electrical grid.

The next figures show how the current flowing through the AC side of the converter varies in the different stages of functioning, the current is considered positive when flowing towards the grid. Here it can also be seen that working in the *qd* frame simplifies the calculations compared to dealing with a sinusoidal signal in the *abc* domain. The higher the power wanted to be exchanged, the higher the current values get.

In the model studied, it can not be observed that the converter has bidirectional power capability, as the device connected to it is a power generator, and it does not make sense that it consumes power. However, this particularity of the converter is important for other applications.

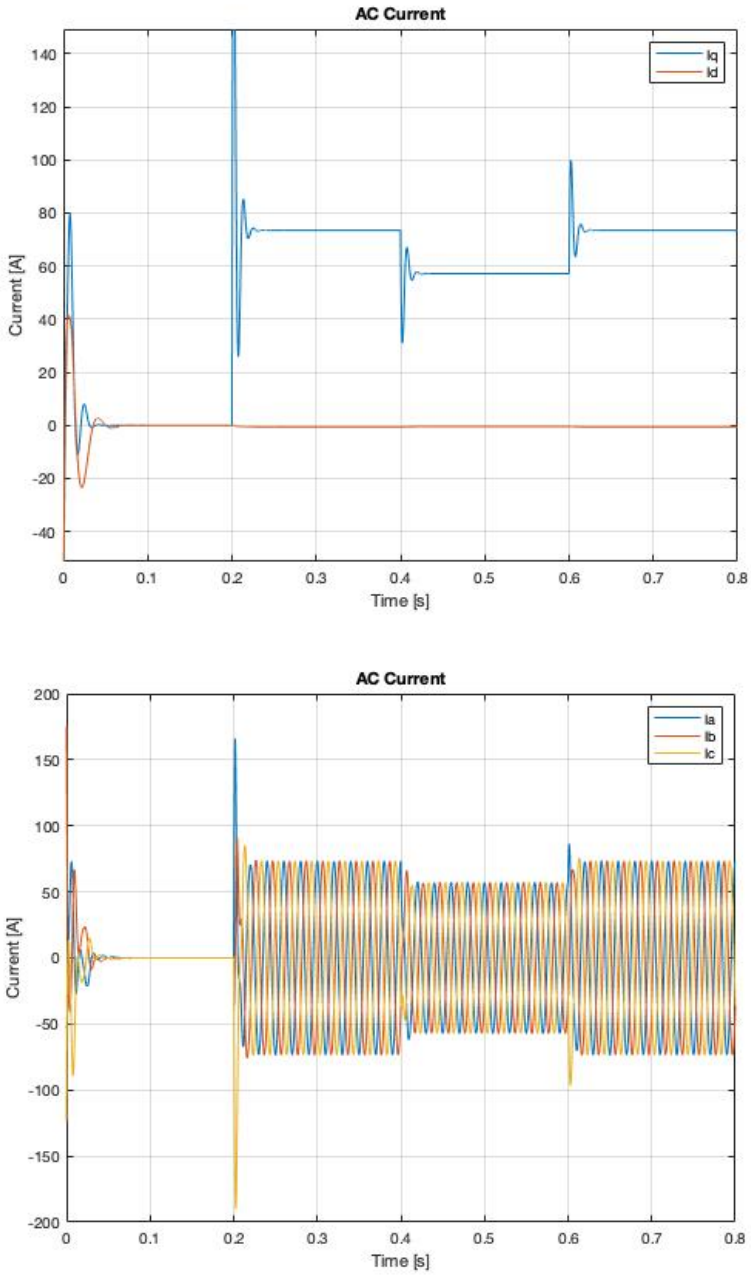

Figure 5.3.1.6. Evolution of the AC side current throughout the simulation in qd and abc domain

Figure 5.3.1.7 shows how the grid and AC side voltages vary throughout the simulation. Voltages measured at the grid side maintain their value during all the simulated period, on the other hand, the converter voltages at the AC side suffer variations.

Converter voltages are imposed by the current loop in order to create the currents that enable power to flow through the converter. Since the grid remains stable and balanced, its voltages stay constant.

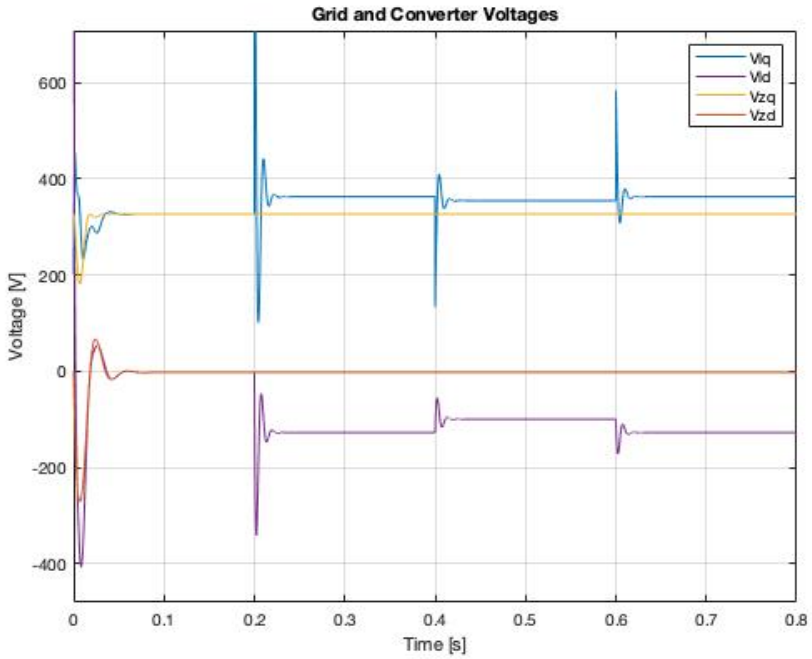

Figure 5.3.1.7. Evolution of the grid and converter AC side voltages throughout the simulation

The results of the simulation are consistent with how the converter was expected to function during the different phases of work.

- In the first stage, there is no power needed to be exchanged, thus, no current flows through the converter and there is no difference between voltages from the grid and the converter. Since it is the start of the simulation, it takes some time for the different variables of the model to settle to their correct values.
- Secondly, the converter enables the PV array to generate the maximum power it can produce in the given conditions. Consequently, a positive current is obtained and a difference between the voltages can be observed. The signals also go through a transient state in the initial instants of this stage, this transient state is fast enough for the converter to function as it is expected to.
- 0.4 seconds into the simulation, the power set-point is decreased, so in this situation, the converter forces the PV array to work in a point that is not the optimal for its generation. In this circumstances there is a part of the potential power generated that is wasted, but this is a common situation that can occur in reality, and it is interesting to see how the model reacts to it.
- Finally, the power generated is again set to 36 kW and all the converter variables are re-established.

5.3.2. Scenario 2

In this second scenario, two different P-V curves are needed, each one in different weather conditions. The first one has been determined in the previous simulation scenario, corresponding to Standard Testing Conditions, and the second curve answers to a different irradiance and temperature values. *Figure 5.3.2.1* shows the two Power-Voltage curves.

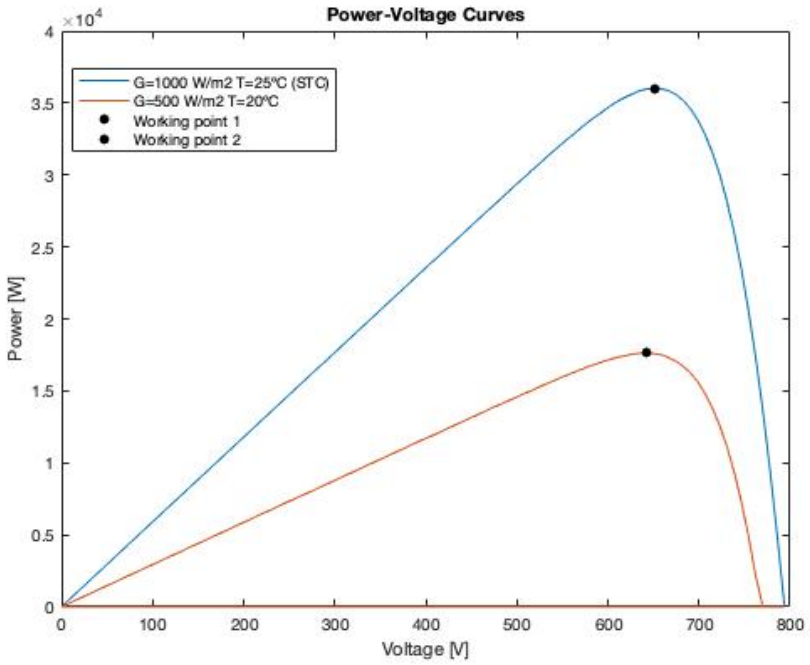

Figure 5.3.2.1. Power-Voltage curves under the two conditions considered and the system working points

For this new case, the inputs for the Simulink model are also the active power set-points, together with the Power-Voltage equations found in the last step. The following table defines the simulation layout.

Time [s]	Desired Active Power [kW]	Voltage [V]
0 - 0.2	36	651
0.2 - 0.4	17.6	643
0.4 - 0.6	36	651

Table 5.3.2.1. Active power input values for the first simulation scenario

Now the simulation can be carried out, and the results are analyzed next.

In the first place, it is interesting to observe how the active power flowing through the converter changes when different set-points are introduced, *Figure 5.3.2.2* shows that the system delivers the desired power to the grid. Even though the weather conditions change, the converter is capable of imposing the voltage that will enable the PV array to

produce the maximum power available in the given conditions. In *Figure 5.3.2.3* it can be seen that the bus voltage at the DC side of the converter always corresponds to the voltages where the P-V curve reaches its maximum.

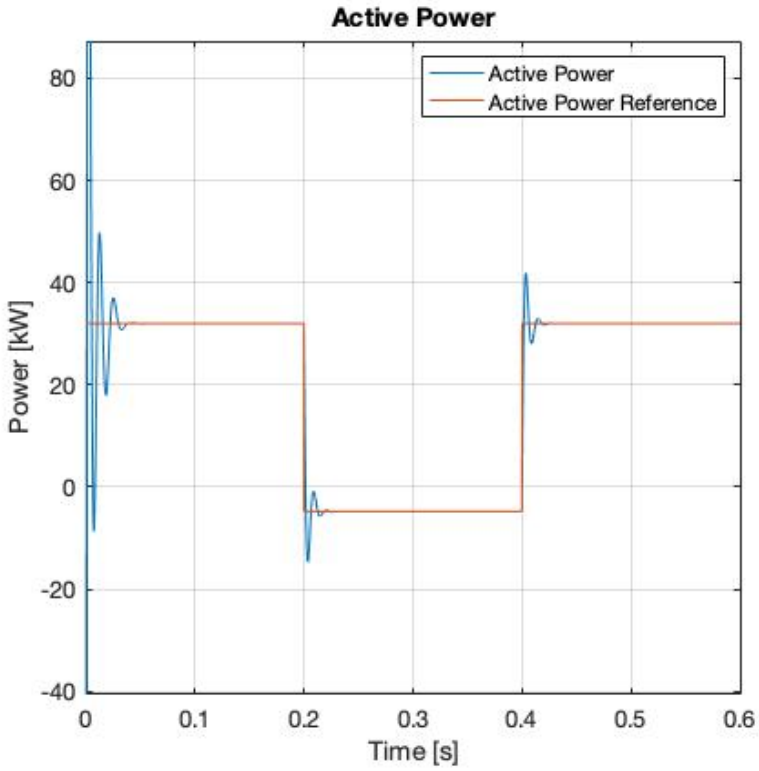

Figure 5.3.2.2. Evolution of the active power throughout the simulation

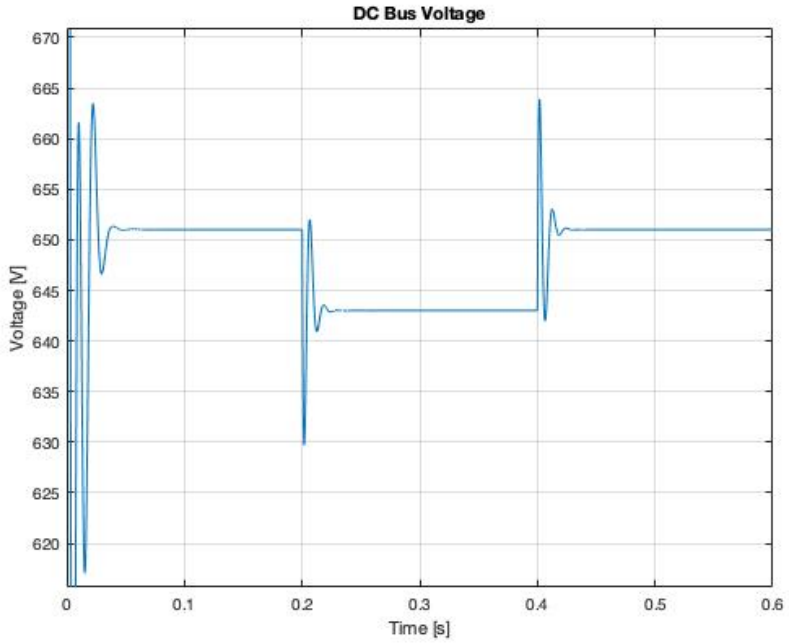

Figure 5.3.2.3. Evolution of the DC bus voltage throughout the simulation

Figure 5.3.2.4 represents the currents flowing through the converter in the *qd* and *abc* frames, currents and voltages represented in the Park domain are used by the control loops, while the measurements made from the converter itself are in the oscillatory abc domain. Here it can be noticed that both domains represent the same magnitudes in different forms.

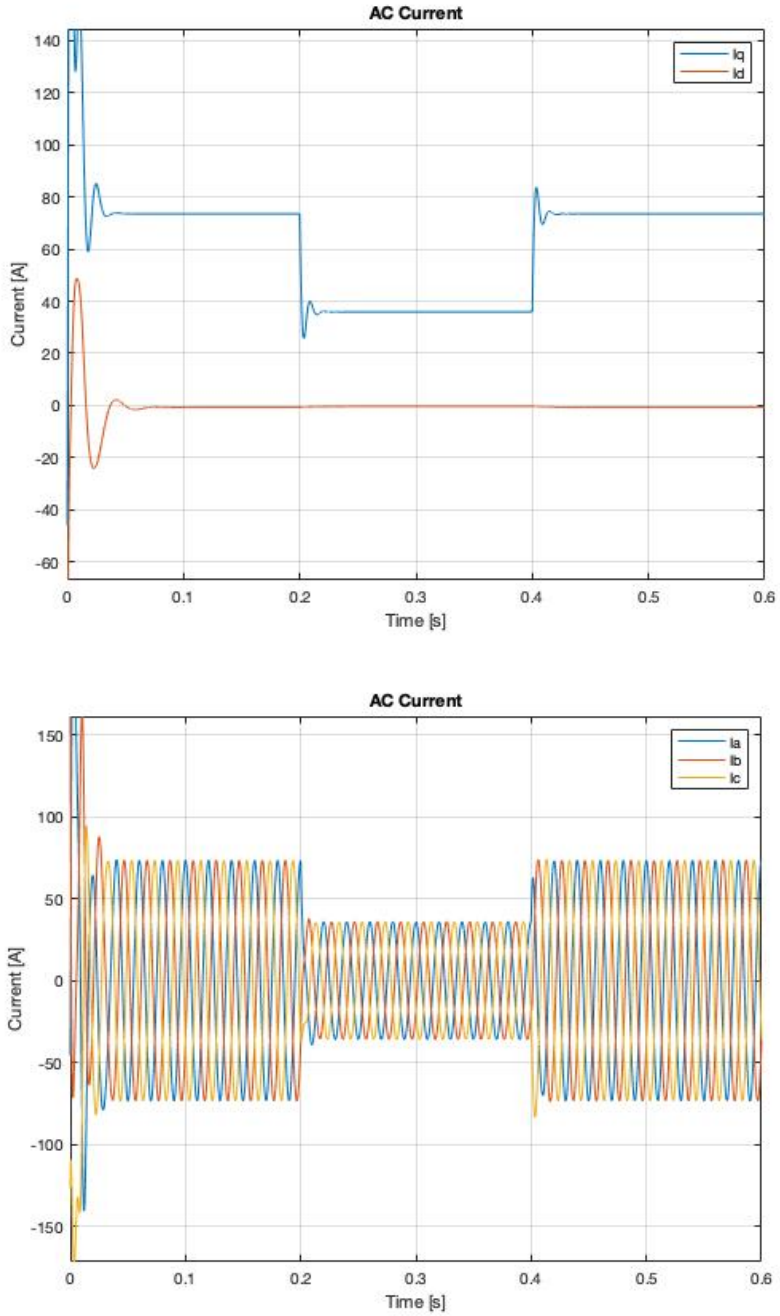

Figure 5.3.2.4. Evolution of the AC side current throughout the simulation in qd and abc domain

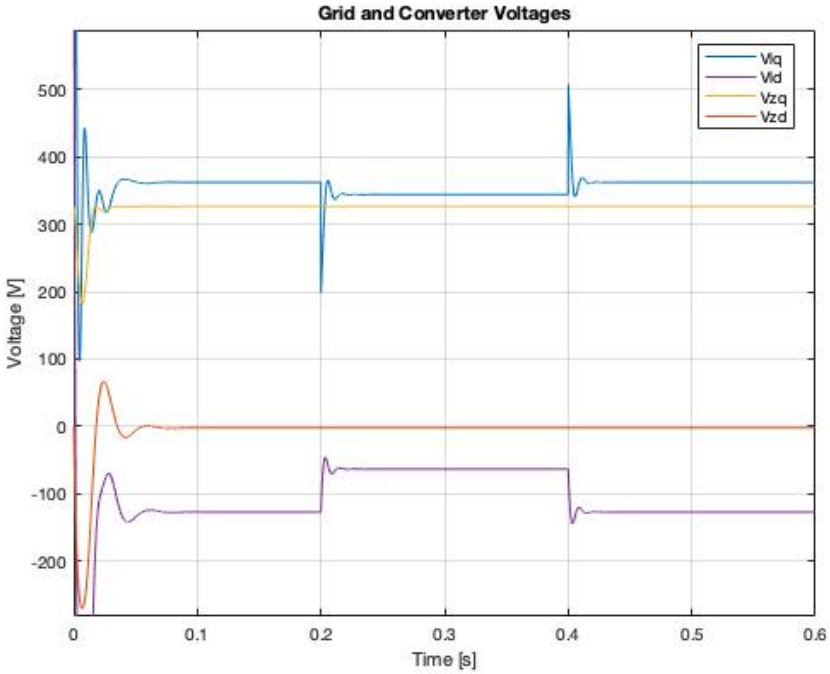

Figure 5.3.2.5. Evolution of the grid and converter AC side voltages throughout the simulation

To conclude with the results analysis, a recap of the simulation stages is made:

- In the beginning, the PV array generates the maximum power that is available in STC and this power transfers to the grid through the converter.
- After 0.2 seconds, the irradiance and temperature conditions are changed, modifying the P-V curve for the photovoltaic array, in this situation. In this new situation, the maximum generated power is achieved when the array is subjected to a different voltage, so the converter regulates the voltage and ensures that the array is working as efficiently as possible.
- At last, STC conditions are restored and all the converter variables take the values that had before in the first phase.

Unlike the previous scenario, here the converter makes sure that the maximum power is generated under any weather condition, constantly taking the most out of the PV array.

6. ENVIRONMENTAL IMPACT

The energy sector is one of the most relevant when it comes to environmental impact. Studies show that nowadays, more than 40% of the electric generation comes from sources that generate polluting waste [11].

The environmental impact of the PV and converter installation can be analyzed from two different scopes. The direct effects of the installation, and the indirect effects, regarding the use of the energy generated by the installation.

Fist the direct effects are studied. Installing an array of solar panels together with a power converter implies the alteration of the terrain where it is going to be installed. Compared to other renewable energy sources, PV cells can be installed almost anywhere, inside urban areas, the most common location are rooftops. Those areas are usually not used before installing the cells, so the impact of building in a PV array in a city or town is less detrimental than doing it in rural areas. Nevertheless, the impact of installing PV cells is less detrimental than other renewable sources, such as wind power.

Next, the indirect effects are analyzed. The generation of energy by PV panels does not generate polluting emissions to the atmosphere and does not contribute to the greenhouse effect. The manufacturing process of the panels and the recycling of those also need to be taken into account when studying the environmental impact. The mentioned processes should be designed to reduce as much as possible the energy used and the waste produced.

Overall, the installation of PV cells and a VSC converter as a energy source has a positive impact, meaning that it is beneficial towards the environment when compared to the conventional more common alternatives for energy generation that are used nowadays.

7. ECONOMIC STUDY

In this chapter, the budget for this project is calculated. This budget pretends to be an approximation to the costs of completing the project, taking into account the different resources used. The resources classify into three categories: equipment, software and labor.

The project was started on February 2019 and finished on September 2019.

Concept	Price per unit	Units	Total
Office equipement	1100 €	1	1100 €
Office	69 €/year	1	69 €
Matlab License for academic research	69 €/year	1	69 €
Simscape Electrical extension	20 €/year	1	20 €
IEEE subscription	27.85 €/article	15	417.75 €
Engineer salary	30 €/hour	400	12000 €
Total			13675.75 €

Table 7.1. Classification of the project costs

The total cost of the project is 13675.75 €.

8. CONCLUSIONS

Nowadays, simulation is essential for reducing time and costs as an alternative to experimental testing. The demand for more reliable and better models that represent any kind of system is rapidly growing. For that reason, once completed the project, a series of conclusions have been obtained.

The obtained PV model is a useful tool for obtaining the Current-Voltage and Power-Voltage curves of any array under different weather conditions. Obtaining the optimal working point is the main objective of modeling the cell behavior, and this can be easily done once the P-V curve is obtained from the model.

Modeling a voltage source converter has been the main objective of this thesis. Observing the simulation results, it can be concluded that the model successfully characterises the performance of a VSC. Experimental testing should be carried out in order to verify the model and ensure that all the results are correct before using the model for any real application.

In the simulation performed it has ben demonstrated that both models can be used together in order to simulate a bigger system. This shows that any of the two models described in this project can be also used in other applications together with new models.

Developing and incorporating any of the models into further studies is clearly a line of work for the future.

9. BIBLIOGRAPHY

[1] Hassan Farhangi. *The path of the smart grid.* IEEE Power and Energy Magazine, 2010.

[2] Trevor Morgan. *Smart Grids and Electric Vehicles: Made for each other?* International Transport Forum, 2012.

[3] APRICUS. *How a PV module works.* http://www.apricus.com, 2019.

[4] Sebastian Valeriu Hudisteanu, Theodor Dorin Mateescu and Catalin George Popovici. *Five parameter model of photovoltaic panel implemented in Matlab/Simulink.* Technical University of Iasi, 2015.

[5] Marcelo Gradella Villalva, Jonas Rafael Gazoli, and Ernesto Ruppert Filho. *Comprehensive Approach to Modeling and Simulation of Photovoltaic Arrays.* IEEE Transactions on Power Electronics, 2009.

[6] Canadian Solar. *Superpower CS6K-300/305/310/315MS Data-sheet.* http://canadiansolar.com, 2015.

[7] Agustí Egea-Alvarez, Adrià Junyent-Ferré and Oriol Gomis-Bellmunt. A*ctive and reactive power control of grid connected distributed generation systems.* CITCEA-UPC.

[8] Eduardo Prieto and Oriol Gomis. *Principles for power electronics based generation* (Slides). CITCEA-UPC.

[9] U. Kamnarn, Y. Kanthaphayao, and V. Chunkag. *Three-phase ac to dc converter with minimized dc bus capacitor and fast dynamic response.* 7th International Conference on Power Electronics and Drive Systems, 2007.

[10] Electronic tutorials. *Phasor diagrams and phasor algebra.* https://www.electronics-tutorials.ws, 2019.

[11] Deloitte. *Recomendaciones para la descarbonización del transporte en España*. https://www.deloitte.com/, 2019.